ORIGINAL ARTICLE

WILEY Plant, Cell & Environment

Estimating stomatal and biochemical limitations during photosynthetic induction

Ross M. Deans [ID] | Graham D. Farquhar [ID] | Florian A. Busch [ID]

ARC Centre of Excellence in Translational Photosynthesis, Division of Plant Science, Research School of Biology, Australian National University, Canberra ACT 2601, Australia

Correspondence
Florian A. Busch, ARC Centre of Excellence in Translational Photosynthesis, Division of Plant Science, Research School of Biology, Australian National University, Canberra, ACT 2601, Australia.
Email: florian.busch@anu.edu.au

Abstract

Understanding stomatal and biochemical components that limit photosynthesis under different conditions is important for both the targeted improvement of photosynthesis and the elucidation of how stomata and biochemistry affect plant performance in an ecological context. Limitation analyses have not yet been extensively applied to conditions of photosynthetic induction after an increase in irradiance. Moreover, few studies have systematically assessed how well various limitation analyses actually work. Here we build on two general ways of estimating limitations, one that sequentially removes the effect of a limitation (elimination) and one that uses a tangent plane approximation (differential), by including the ternary effect and boundary layer conductance so that they are consistent with gas exchange data. We apply them to the analysis of temporal and time-integrated limitations during photosynthetic induction, calculating limitations either independent of the time course (one-step) or make use of the entire time course (stepwise). We show that the stepwise differential method is the best method to use when time steps are small enough. We further show that the differential method predicts limitations near exact when the internal CO_2 concentration stays constant. This last insight has important implications for the general use of limitation analyses beyond photosynthetic induction.

KEYWORDS

biochemical activation, kinetics of stomatal responses, light, limitations, photosynthesis, photosynthetic induction, stomata

1 | INTRODUCTION

Identifying photosynthetic limitations of a plant is integral to understanding the functioning of a plant in its environment. Limitation analyses address how various components limit photosynthesis (Jones, 1985). Not only can limitations provide insights into photosynthetic physiology under different conditions and in different genotypes, but they can also hint at where a plant should invest to gain the greatest benefit in photosynthesis. The major photosynthetic limitations at the leaf level can be broadly split into the restriction of CO_2 supply to the site of carboxylation by diffusional effects and limitations in the consumption of CO_2 by biochemical effects (Jones, 1973; Jones, 1985). Diffusional limitations can be further separated into stomatal effects limiting CO_2 supply into the leaf and mesophyll effects limiting CO_2 supply from the intercellular airspace to the site of carboxylation (Grassi & Magnani, 2005), whereas biochemical effects include the maximum rate of carboxylation by Rubisco and the capacity for regeneration of RuBP in the Calvin–Benson cycle (Busch & Sage, 2017; Farquhar, von Caemmerer, & Berry, 1980).

Increasing the speed of photosynthetic induction under dynamic light environments has been suggested as a possible way to increase crop photosynthesis (Kaiser et al., 2015; Kaiser, Morales, & Harbinson, 2018; Kromdijk et al., 2016; Lawson & Blatt, 2014; McAusland et al., 2016; Slattery, Walker, Weber, & Ort, 2018; Taylor & Long, 2017). In response to an increase in irradiance, photosynthesis does not achieve its final value instantaneously but exhibits a delay. Thus, a leaf

transiently forgoes potential photosynthesis compared with the assimilation rate reaching steady state instantaneously (Deans, Brodribb, Busch, & Farquhar, 2019). In a dynamic sense, a photosynthetic limitation at the leaf level can be defined as a reduction in the total photosynthesis achieved compared with that obtained if photosynthesis had reached its final value instantaneously, caused by both biochemical and diffusional effects (Figure 1a). Firstly, photosynthesis is limited by the necessary build-up of Calvin-cycle intermediates and the slow induction of light-activated photosynthetic enzymes immediately following the increase in irradiance (Mott & Woodrow, 2000).

Build-up of the RuBP pool typically limits photosynthesis for approximately 60 s following an increase in irradiance, whereas full light activation of Rubisco typically takes 8–10 min (Mott & Woodrow, 2000). Secondly, photosynthesis is limited by the supply of CO_2 through slow stomatal opening (Kirschbaum & Pearcy, 1988). Although some stomata respond rapidly following an increase in irradiance (e.g. in some monocot species), stomata can take much longer to fully open, potentially posing a significant photosynthetic limitation (Deans et al., 2019; McAusland et al., 2016; Vico, Manzoni, Palmroth, & Katul, 2011). Finally, mesophyll conductance has been shown to increase
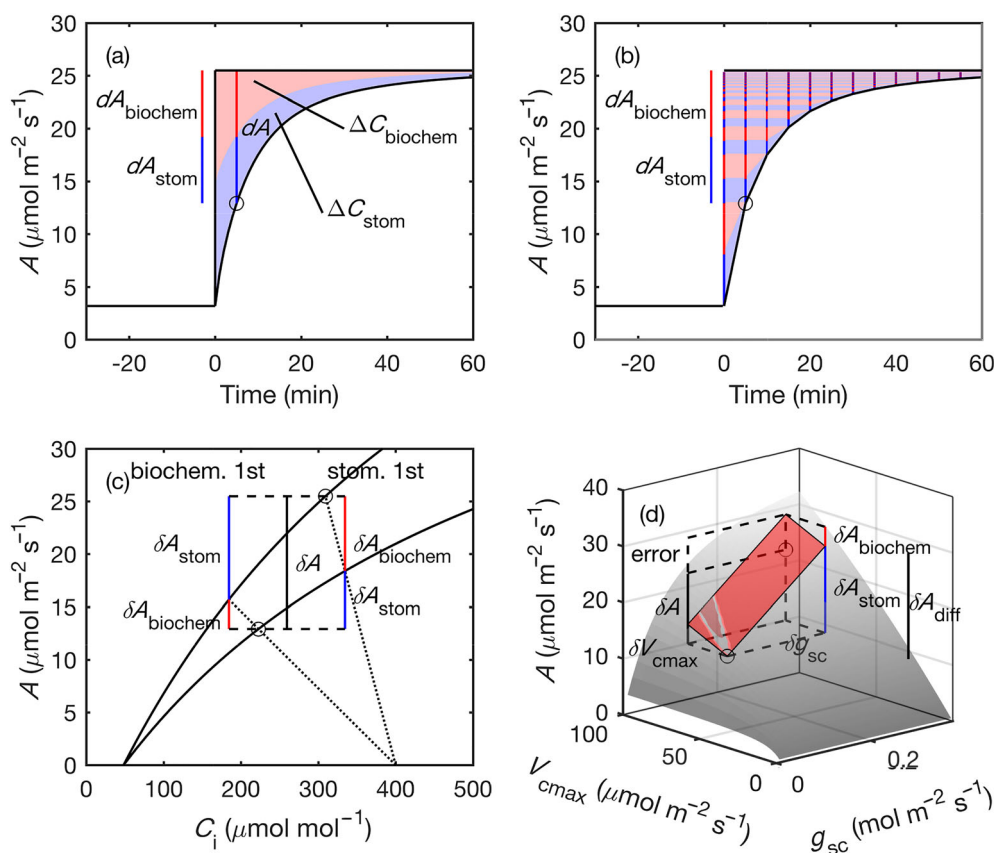

FIGURE 1 Methods and approaches to calculating stomatal and biochemical limitations during photosynthetic induction. (a) Calculating limitations using the one-step approach. Following an increase in irradiance at time = 0 min, A increases slowly due to delayed biochemical activation and stomatal opening, resulting in plants not achieving the potential assimilation rate that would occur if stomatal opening and biochemical activation had reached their final values instantaneously (dA). Limitation analyses aim to separate this difference in photosynthesis into biochemical ($dA_{biochem}$, red) and stomatal (dA_{stom}, blue) effects. In the one-step approach, limitations are calculated directly. Similarly, they can also separate total assimilation forgone during induction (coloured area above curve) into biochemical ($\Delta C_{biochem}$, light red) and stomatal (ΔC_{stom}, light blue) effects. (b) Calculating limitations using the stepwise approach. This approach calculates limitations to the next time point. The limitation at the current time point is then the sum of all future limitation steps back to the current timepoint. (c) Calculation of limitations using the elimination methods, illustrated on an A vs. C_i curve. The two black curves represent A vs. C_i curves for V_{cmax} at the first (lower curve) and second (upper curve) photosynthetic state. Dotted lines represent CO_2 supply curves, governed by the stomatal conductance in the first (lower line) and second (upper line) photosynthetic states. Removal of the biochemical limitation first (left side) involves tracking along the current CO_2 supply line to the final A vs. C_i curve, the difference in A from the first state being $dA_{biochem}$ (red). dA_{stom} (blue) is the remaining difference from the second A. Removal of the stomatal limitation first (right side) involves following the current A versus C_i curve until the second CO_2 supply line is reached, the difference in A from the first state being dA_{stom} (blue). $dA_{biochem}$ (red) being the remaining difference from the final A. The estimates of biochemical and stomatal limitations are dependent on the order limitations are removed. (d) Calculation of limitations using the differential method. The light grey surface is the 'assimilation surface' A (V_{cmax}, g_{sc}). Open circles show the first and second photosynthetic states. A tangent plane (red plane) is projected tangential to the surface at the current point and biochemical ($dA_{biochem}$, red) and stomatal (dA_{stom}, blue) components of dA are constructed by traversing the plane between current and final V_{cmax} (dV_{cmax}) and g_{sc} (dg_{sc}), respectively, and calculating the difference in A between these points and the first photosynthetic state. The sum of $dA_{biochem}$ and dA_{stom} corresponds to the predicted difference in A (dA_{diff}). The difference between the predicted and actual dA is the error

with irradiance (Douthe, Dreyer, Brendel, & Warren, 2012; Douthe, Dreyer, Epron, & Warren, 2011; Flexas, Ribas-Carbo, Diaz-Espejo, Galmes, & Medrano, 2008). These changes in mesophyll conductance occur rapidly, in the order of minutes (Douthe et al., 2011). However, changes in mesophyll conductance with changing irradiance are not universal across species (Tazoe, von Caemmerer, Badger, & Evans, 2009). Variable mesophyll conductance potentially poses another significant limitation to photosynthesis in dynamic light environments.

Despite the overall effects of photosynthetic limitations being clearly apparent during photosynthetic induction, few studies have utilized photosynthetic limitation analyses to quantify the contributions of biochemical and diffusional limitations in this setting (Taylor & Long, 2017). Limitation analyses also typically utilize simplified equations that ignore the ternary correction and boundary layer conductance (von Caemmerer & Farquhar, 1981). The ternary effect takes into account the diffusion of CO_2 in water vapour (Jarman, 1974), whereas the boundary layer conductance accounts for the extra resistance of the boundary layer in the diffusion of gas from the leaf surface to the surroundings. Although these effects are normally only significant at high transpiration rates and stomatal conductances, respectively, gas exchange data are typically calculated including both effects. Here we derived equations for two methods to calculate limitations including these effects and applied them during photosynthetic induction. The first, an elimination method, calculates limitations by removing the effect of each limitation sequentially (Assmann, 1988; Jones, 1985; Wilson, Baldocchi, & Hanson, 2000). The second, a differential method, allocates limitations by linearizing the impact of each limitation on assimilation rate (Grassi & Magnani, 2005; Jones, 1985; Wilson et al., 2000). We estimated both the temporal dynamics of absolute limitations, as well as time-integrated relative photosynthetic limitations during photosynthetic induction, on a set of 42 such inductions from Deans et al. (2019), comprising 15 species. We did this for both methods in two different ways: a stepwise method that took into account previous and subsequent limitation estimates and a one-step method that did not. Our aim was to systematically compare the performance of the different ways of estimating limitations during photosynthetic induction and to determine what method is best to use and when.

2 | THEORY

As described in Deans et al. (2019), following an increase in irradiance from low light or darkness, slow biochemical activation and stomatal opening limits the rate of photosynthesis the plant can achieve compared with the final steady-state photosynthetic rate. This instantaneous difference in photosynthetic rate (dA) is defined as

$$dA(t) = A_f - A(t), \tag{1}$$

where A_f is the final assimilation rate at steady state and $A(t)$ is the current assimilation rate at time t.

It is also interesting to know how much total assimilation the plant forgoes during photosynthetic induction. Forgone assimilation (ΔC) is defined as

$$\Delta C = \int_0^{t_f} dA(t) dt = \int_0^{t_f} (A_f - A(t)) dt, \tag{2}$$

where t_f is the time corresponding to A_f and the change in irradiance occurs at $t = 0$.

The aim of the limitation analyses here is to separate dA and ΔC into stomatal and biochemical components. To do so requires the calculation of limitation estimates on dA at each time point. There are two ways that this can be done. The first, here called a one-step method, calculates the limitation from the final A directly (Figure 1a). It is computationally simpler, but large errors may be expected if the final A state is far from the current state. This approach is closer to state function approaches for the estimate of limitations because the current limitation of dA is calculated without knowledge of the limitations affecting neighbouring time points (Jones, 1985). The second, here called a stepwise method, calculates the limitation to the next time point, and then the limitation of dA is calculated by summing all the limitation components from the final time point back to the current one (Figure 1b). This method is computationally more demanding, but error in limitation estimates may be expected to be smaller provided time steps between points is small enough. This method is a path-dependent method because knowledge of limitations throughout the time course of induction is used to calculate the current limitation (Jones, 1985).

Calculation of biochemical and stomatal limitation during photosynthetic induction require an expression for A in terms of the component limitations. Biochemical limitations during photosynthetic induction are predominantly caused by Rubisco activation, with ribulose-1,5-bisphosphate (RuBP) regeneration only limiting for less than 1 min after an increase in irradiance (Mott & Woodrow, 2000). It is instructive then to consider A as a function of the maximum carboxylation rate of Rubisco in the current activation state (V_{cmax}) and stomatal conductance to CO_2 (g_{sc}), that is,

$$A(t) \equiv A(V_{cmax}(t), g_{sc}(t)).$$

We note here that $g_{sc} = g_{sw}/1.6$, where g_{sw} is the stomatal conductance to water vapour, the more commonly calculated stomatal conductance in gas exchange systems. The factor 1.6 takes into account the ratio of the diffusivities of water and CO_2 in air.

An expression for A is required in terms of V_{cmax} and g_{sc}. The Rubisco-limited biochemistry of photosynthesis can be described by (Farquhar et al., 1980)

$$A = \frac{V_{cmax}\left(C_i - \Gamma^*\right)}{C_i + K_m} - R_d, \tag{3}$$

where C_i is the CO_2 concentration in the intercellular airspace, Γ^* is the CO_2 compensation point in the absence of respiration, K_m is the effective Michaelis–Menten constant taking into account the O_2 concentration and R_d is the rate of mitochondrial respiration in the light.

Here it was assumed that the CO_2 concentration at the site of carboxylation was equal to C_i because steady state and dynamic mesophyll conductance were not consistently known in the plants sampled.

An equation for C_i is required. From von Caemmerer and Farquhar (1981), C_i including the ternary correction is

$$C_i = \frac{C_a\left(g_{tc} - \frac{E}{2}\right) - A}{\left(g_{tc} + \frac{E}{2}\right)}, \tag{4}$$

where C_a is the ambient CO_2 concentration and g_{tc} is the total conductance to CO_2 from outside the leaf boundary layer to inside the leaf. g_{tc} can be further broken up into

$$g_{tc} = \frac{g_{sc}g_{bc}}{g_{sc} + g_{bc}}, \tag{5}$$

where g_{bc} is the boundary layer conductance to CO_2.

Substituting Eqn 4 into Eqn 3 and rearranging gives

$$A^2 - \left[V_{cmax} - R_d + C_a\left(g_{tc} - \frac{E}{2}\right) + K_m\left(g_{tc} + \frac{E}{2}\right)\right]A$$
$$+ V_{cmax}\left[C_a\left(g_{tc} - \frac{E}{2}\right) - \Gamma^*\left(g_{tc} + \frac{E}{2}\right)\right] - R_d\left[C_a\left(g_{tc} - \frac{E}{2}\right) + K_m\left(g_{tc} + \frac{E}{2}\right)\right]$$
$$= 0. \tag{6}$$

A thus has the solution

$$A = \left(\frac{1}{2a}\right)\left(b - \sqrt{b^2 - 4ac}\right), \tag{7}$$

where

$$a = 1, \tag{7a}$$

$$b = V_{cmax} - R_d + C_a\left(g_{tc} - \frac{E}{2}\right) + K_m\left(g_{tc} + \frac{E}{2}\right), \tag{7b}$$

and

$$c = V_{cmax}\left[C_a\left(g_{tc} - \frac{E}{2}\right) - \Gamma^*\left(g_{tc} + \frac{E}{2}\right)\right] - R_d\left[C_a\left(g_{tc} - \frac{E}{2}\right) + K_m\left(g_{tc} + \frac{E}{2}\right)\right]. \tag{7c}$$

The two methods to calculate limitations will rely on Eqns 3, 5, 6 and 7 in both the derivations and calculations of limitations.

2.1 | Elimination methods

Elimination methods sequentially remove the effect of one limitation and calculate the resulting difference in assimilation until all limitations have been accounted for (Jones, 1973; Jones, 1985). However, the nonlinear nature of photosynthesis means that there is often not a unique solution and that a different solution will be obtained depending on the order that the limitation effects are removed (Figure 1c). It is for this reason that it is referred to as a path-dependent method (Jones, 1973). Considering dynamic changes in V_{cmax}, g_{sc} and E only, and if V_{cmax1}, g_{sc1} and E_1, and V_{cmax2}, g_{sc2} and E_2 are the V_{cmax}, g_{sc}

and E at two photosynthetic states, respectively, then there are two ways of calculating the respective limitations:

1. Removing the stomatal limitation first gives

$$\delta A_{stom,stom} = A(V_{cmax1}, g_{sc2}, E_2) - A(V_{cmax1}, g_{sc1}, E_1) \tag{8}$$

and

$$\delta A_{biochem,stom} = A(V_{cmax2}, g_{sc2}, E_2) - A(V_{cmax1}, g_{sc2}, E_2), \tag{9}$$

where the first subscript of δA indicates the limitation and the second indicates which limitation was eliminated first.

2. Removing the biochemical limitation first gives

$$\delta A_{biochem,biochem} = A(V_{cmax2}, g_{sc1}, E_1) - A(V_{cmax1}, g_{sc1}, E_1) \tag{10}$$

and

$$\delta A_{stom,biochem} = A(V_{cmax2}, g_{sc2}, E_2) - A(V_{cmax2}, g_{sc1}, E_2). \tag{11}$$

The intermediate assimilation rates are calculated using Eqn 7, substituting in the relevant values for V_{cmax}, g_{sc} and E as required. A graphical example of the two elimination approaches is illustrated in Figure 1c.

Using the one-step method of calculating limitations, State 1 is the current time point and State 2 is the final time point and

$$dA_{x,y}(t) = \delta A_{x,y}(t), \tag{12}$$

where x is the limitation and y is the limitation that was removed first.

Using the stepwise method, State 1 is the current time point and State 2 is the next time point. $dA_{x,y}$ for the current time point is then calculated as

$$dA_{x,y}(t) = \sum_{i=t}^{t_f} \delta A_{x,y}(i), \tag{13}$$

where i is a dummy variable for t.

The time-integrated relative limitation over the duration of photosynthetic induction ($\sigma_{x,y}$) was calculated by integrating the calculated $dA_{x,y}$ over the time course and dividing by forgone assimilation, ΔC, that is,

$$\sigma_{x,y} = \frac{1}{\Delta C}\int_0^{t_f} dA_{x,y}(t)dt, \tag{14}$$

where the integration is again done from the time of change in irradiance ($t = 0$) to time $t = t_f$, the time corresponding to the final assimilation rate A_f.

Typically, limitations should range between 0 and 1; for example, a $\sigma_{stom,biochem}$ of 0.4 indicates 40% of the forgone photosynthesis during photosynthetic induction was due to slow stomatal opening, whereas

60% was due to slow biochemical activation, when evaluated removing the biochemical limitation first. However, values for limitations <0 or >1 are possible and represent occasions where g_{sc} and/or V_{cmax} are transiently greater than their final values at some point during photosynthetic induction. For example, if stomata transiently overshoot the final g_{sc} value, then stomata become less limiting than if g_{sc} was at the final steady state value, and the value for, say, $dA_{stom,biochem}$ would become negative. If the overshoot occurs for long enough then $\Delta C_{stom,biochem}$ may also become negative, but if V_{cmax} is rising monotonically to its final value then $\Delta C_{biochem,biochem}$ would be positive and greater than ΔC by definition. Thus $\sigma_{stom,biochem}$ would be <0 and $\sigma_{biochem,biochem}$ would be >1. In this scenario, if ΔC is small compared with the component limitations, poorer estimates of time-integrated relative limitations may be expected.

From the elimination method, we obtain two potentially different estimates of limitations depending on which limitation is removed first. It is instructive then to consider the mean and a range estimate of the limitations calculated. The mean component of dA due to a limitation x (i.e. stomatal or biochemical) at each time point ($dA_{x,mean}$) was defined as

$$dA_{x,mean} = \frac{1}{2}(dA_{x,stom} + dA_{x,biochem}).$$ (15)

The mean time-integrated limitation ($\sigma_{x,mean}$) is then

$$\sigma_{x,mean} = \frac{1}{2}(\sigma_{x,stom} + \sigma_{x,biochem}).$$ (16)

The relative range in dA for the elimination method ($rel.range(dA)_{elim}$) was defined as the absolute value of the difference between the two estimates of a limitation, divided by the instantaneous difference in photosynthetic rate (dA), that is,

$$rel.range(dA)_{elim} = \frac{|dA_{x,y} - dA_{x,x}|}{|dA|},$$ (17)

where x and y are limitations (i.e. stomatal or biochemical). Similarly, the relative range in ΔC ($rel.range(\Delta C)_{elim}$) can be defined as

$$rel.range(\Delta C)_{elim} = \frac{|\Delta C_{x,y} - \Delta C_{x,x}|}{|\Delta C|},$$ (18)

where

$$\Delta C_{x,y} = \int_0^{t_f} dA_{x,y}(t)dt.$$ (19)

It is shown in Data S1 in the Supporting Information that the relative range estimates are identical whether the range is calculated using the stomatal or biochemical limitations.

2.2 | Differential method

The differential method uses a linear approximation to calculate the effect of limitations on photosynthesis (Deans et al., 2019; Grassi & Magnani, 2005; Jones, 1973; Jones, 1985; Wilson et al., 2000).

Ignoring the ternary effect for now, we can consider $A(V_{cmax}, g_{sc})$ as an 'assimilation surface', and $A_1 = A(V_{cmax1}, g_{sc1})$ and $A_2 = A(V_{cmax2}, g_{sc2})$, as two points on the surface (Figure 1d). $A(t)$ tracks a path on the assimilation surface through time as photosynthetic induction occurs. Because A is a nonlinear surface, we cannot directly calculate the component that each limitation contributes to δA; however, δA can be linearized using a Taylor series. Below we derive the differential method including both the ternary correction and boundary layer conductance.

Following Deans et al. (2019), δA can be linearized as

$$\delta A = \frac{\partial A}{\partial V_{cmax}}\delta V_{cmax} + \frac{\partial A}{\partial g_{sc}}\delta g_{sc} + error,$$ (20)

where the partial derivatives are evaluated at State 1, and δV_{cmax} and δg_{sc} are the differences in the respective variables between State 2 and State 1. We can depict this linearization as a tangent plane that touches the assimilation surface at the current state (Figure 1d). Individual differences in assimilation can be identified as

$$\delta A_{biochem} = \frac{\partial A}{\partial V_{cmax}}\delta V_{cmax}$$ (21)

and

$$\delta A_{stom} = \frac{\partial A}{\partial g_{sc}}\delta g_{sc},$$ (22)

where $\delta A_{biochem}$ and δA_{stom} are the components of δA due to biochemical and stomatal limitations, respectively.

It is noted here that the single-point calculation of limitations using a control coefficient or sensitivity analysis is a special case of the two-point limitation analysis, where one point is taken as zero (Jones, 1985; Woodrow & Berry, 1988), that is,

$$s_{Vcmax} = \frac{\partial A}{\partial V_{cmax}}\frac{V_{cmax}}{A}$$

and

$$s_{gsc} = \frac{\partial A}{\partial g_{sc}}\frac{g_{sc}}{A},$$

where s_{Vcmax} and s_{gsc} are the sensitivity or control coefficient for respective limitations.

The calculation of each limitation requires the evaluation of the partial derivatives of A with respect to V_{cmax} and g_{sc}. We appeal to Eqn 6, calculating derivatives implicitly. Differentiating Eqn 6 with respect to V_{cmax} and substituting into Eqn 21 gives

$$\delta A_{biochem} = \frac{C_a\left(g_{tc} - \frac{E}{2}\right) - \Gamma^*\left(g_{tc} + \frac{E}{2}\right) - A}{\left[V_{cmax} - R_d + C_a\left(g_{tc} - \frac{E}{2}\right) + K_m\left(g_{tc} + \frac{E}{2}\right) - 2A\right]}\delta V_{cmax}.$$ (23)

Differentiating Eqn 6 with respect to g_{sc} is more complicated, as altering g_{sc} will have an effect on E. The ternary-corrected equation for E is

$$E = \frac{g_{tw}(w_i - w_a)}{\left[1 - \frac{(w_i + w_a)}{2}\right]}, \tag{24}$$

(von Caemmerer & Farquhar, 1981) where g_{tw} is the total conductance to water vapour, and w_i and w_a are the water mole fractions inside and outside the leaf, respectively. g_{tw} can be expressed as

$$g_{tw} = \frac{g_{sw}g_{bw}}{g_{sw} + g_{bw}} = \frac{(1.6g_{sc})(1.37g_{bc})}{1.6g_{sc} + 1.37g_{bc}}, \tag{25}$$

where g_{sw} and g_{bw} are the stomatal and boundary layer conductances to water vapour, respectively. The factor 1.37 interconverting the boundary layer conductances to water vapour and CO_2 comes from a consideration of mass flow in laminar flows (von Caemmerer & Farquhar, 1981).

Further chamber feedbacks of E on w_a are ignored. It can be shown that

$$\frac{\partial\left(g_{tc} \pm \frac{E}{2}\right)}{\partial g_{sc}} = \frac{1}{g_{sc}^2}\left(g_{tc}^2 \pm \frac{g_{tw}E}{1.62}\right), \tag{26}$$

so that

$$\delta A_{stom} = \left(\frac{1}{g_{sc}^2}\right)\frac{C_a[V_{cmax} - (A + R_d)]\left(g_{tc}^2 - \frac{g_{tw}E}{1.62}\right) - \left[V_{cmax}\Gamma^* + K_m(A + R_d)\right]\left(g_{tc}^2 + \frac{g_{tw}E}{1.62}\right)}{\left[V_{cmax} - R_d + C_a\left(g_{tc} - \frac{E}{2}\right) + K_m\left(g_{tc} + \frac{E}{2}\right) - 2A\right]}\delta g_{sc}. \tag{27}$$

The components of δA due to each limitation are calculated using Eqns 23 and 27. For the one-step calculation of limitations, State 1 is the current time point and State 2 is the final time point and

$$dA_x(t) = \delta A_x(t), \tag{28}$$

where x is the limitation.

For the stepwise calculation of limitations, State 1 is the current time point and State 2 is the next time point. dA_x is then calculated as

$$dA_x(t) = \sum_{i=t}^{t_f} \delta A_x(i), \tag{29}$$

where i is again a dummy variable for t.

Neither Wilson et al. (2000) nor Grassi and Magnani (2005) consider the effect of boundary layer conductance or of the ternary correction. They also follow a different route for splitting the effect of limitations, initially noting that changing either C_i or V_{cmax} can change assimilation and then further noting that a change in C_i can occur by changing A or g_{sc}. If the ternary correction and boundary layer conductance are ignored in our analysis (i.e. g_{bc}, g_{bw} and E all set to zero), the two approaches used to derive limitations are identical (see Data S1).

The total assimilation forgone due to a limitation x (either biochemical or stomatal) over the duration of photosynthetic induction can be calculated as

$$\Delta C_x = \int_0^{t_f} dA_x dt. \tag{30}$$

The instantaneous difference in photosynthetic rate estimated by the differential method (dA_{diff}) is

$$dA_{diff} = dA_{biochem} + dA_{stom}, \tag{31}$$

whereas the estimate of forgone assimilation (ΔC_{diff}) is

$$\Delta C_{diff} = \Delta C_{biochem} + \Delta C_{stom}. \tag{32}$$

The time-integrated limitation over the duration of photosynthetic induction (σ_x) is then (Deans et al., 2019)

$$\sigma_x = \frac{\Delta C_x}{\Delta C_{diff}}, \tag{33}$$

where x is the limitation (i.e. biochemical or stomatal).

Unlike the elimination method, there is only one estimate for the effect of each limitation on forgone potential assimilation using the differential method. Instead, linearization introduces an intrinsic error in dA_{diff} and ΔC_{diff}, causing them to differ from dA and ΔC, respectively. We can define the relative error in dA for the differential method ($rel.error(dA)_{diff}$) as

$$rel.error(dA)_{diff} = \frac{|dA - dA_{diff}|}{|dA|}. \tag{34}$$

Likewise for ΔC, we can define the relative error ($rel.error(\Delta C)_{diff}$) as

$$rel.error(\Delta C)_{diff} = \frac{|\Delta C - \Delta C_{diff}|}{|\Delta C|}. \tag{35}$$

3 | METHODS

3.1 | Experimental testing of limitations

The elimination and differential methods of estimating limitations were tested on a data set of 42 time courses of photosynthetic induction following an increase in irradiance from 15 species, from the study of Deans et al. (2019). Species tested were _Adiantum capillus-veneris_, _Austrocedrus chilensis_, _Callitris preissii_, _Dicksonia antarctica_, _Eucalyptus pauciflora_, _Gossypium hirsutum_, _Histiopteris incisa_, _Hypolepis rugolusa_, _Marsilea drummondii_, _Nothofagus cunninghamii_, _Pinus radiata_, _Prumnopitys ladei_, _Spinacea oleracea_ cv. 'Viking', _Vicia faba_ and _Vitis vinifera_ cv. 'Chardonnay' and represent a broad range of stomatal opening times and photosynthetic capacities.

In Deans et al. (2019), gas exchange dynamics were measured using an infrared gas analyser (IRGA; LI-6400XT; LICOR Biosciences, Lincoln, Nebraska, USA), maintaining reference CO_2 concentration and chamber temperature. This meant that C_a in the chamber decreased during photosynthetic induction. For both calculating C_i and in further calculations of limitations at each time point, the C_a at that point in time was used. The response time for the chamber was also ignored, although the small chamber volume relative to leaf

area and system flow rate, the IRGAs being close to the site of gas exchange in this system, and the changes in chamber conditions occurring via plant responses and not step changes in incoming gas composition together mean that the effect is small.

All methods for calculating limitations require an estimate of how V_{cmax} changes throughout photosynthetic induction. V_{cmax} was obtained by rearranging Eqn 3 and solving for V_{cmax}:

$$V_{cmax}(t) = \frac{(A(t) + R_d)(C_i(t) + K_m)}{C_i(t) - \Gamma^*} \qquad (36)$$

R_d was assumed to be the same as dark respiration, whereas Γ^* and K_m were taken as the mean values for C_3 species from Hermida-Carrera, Kapralov, and Galmés (2016) as 41.2 and 529.4 µmol mol^{-1}, respectively, at 25 °C.

Stomatal and biochemical components of dA were estimated at each time point throughout time courses of photosynthetic induction for all 42 traces, comparing the elimination methods (Eqns 8–11) with the differential method (Eqns 23 and 27) using both the one-step (Eqns 12 and 28) and stepwise calculation of limitations (Eqns 13 and 29). This required the calculation of g_{tc} and g_{tw} at each time point using Eqns 5 and 25, respectively. g_{bw} was assumed to be 2.84 mol m^{-2} s^{-1}, the value for the 6 cm^2 chamber with fast fan speed for the LI-6400XT. dA_{diff} was also calculated at each time point for both the one-step and stepwise methods (Eqn 31).

Components of ΔC due to each limitation were calculated for the elimination methods ($\Delta C_{x,y}$; Eqn 19), as was observed forgone assimilation (ΔC; Eqn 2). These were used to calculate time-integrated relative limitations during photosynthetic induction for the elimination methods ($\sigma_{x,y}$; Eqn 14) and the relative range of the elimination methods (rel.range(ΔC)$_{elim}$; Eqn 18). Components of ΔC due to each limitation were calculated for the differential method (ΔC_x; Eqn 30), along with the total forgone assimilation predicted by the differential method (ΔC_{diff}; Eqn 32). These were used to calculate the time-integrated relative limitations during photosynthetic induction for the differential method (σ_x; Eqn 33) and the relative error of the differential method (rel.error(ΔC)$_{diff}$; Eqn 35).

Stomatal opening (t_{90g}) and biochemical activation (t_{90V}) response times were defined as the time to 90% of the difference between the respective initial and maximum values of g_{sc} and V_{cmax}, following Deans et al. (2019).

3.2 | Simulating the relative effect of stomatal opening and biochemical activation times on error in the limitation analyses

Photosynthetic induction following an increase in irradiance was modelled for a range of stomatal opening and biochemical activation times to investigate the effect of each on the relative range of the elimination method and the relative error of the differential method. The increase from low to high irradiance was taken to occur at time $t = 0$ min. For simplicity, biochemical activation and stomatal opening were assumed to follow exponential rise to maximum kinetics in

simulations, despite variation in the dynamic behaviour of photosynthetic induction, that is, for biochemical activation

$$V_{cmax}(t) = V_{cmaxf} + (V_{cmaxi} - V_{cmaxf})e^{-\frac{t}{\tau_V}}, \qquad (37)$$

where V_{cmaxi} and V_{cmaxf} are the initial and final V_{cmax}, respectively, and τ_V is the characteristic time for biochemical activation; and for stomatal opening,

$$g_{sc}(t) = g_{scf} + (g_{sci} - g_{scf})e^{-\frac{t}{\tau_g}}, \qquad (38)$$

where g_{sci} and g_{scf} are the initial and final g_{sc}, respectively, and τ_g is the characteristic time for stomatal opening. t_{90} and τ for both stomatal opening and biochemical activation were interrelated by

$$t_{90} = -\tau \log_e(0.1). \qquad (39)$$

At each time point, E was calculated from Eqn 24, assuming w_i and w_a of 0.032 and 0.022 mol mol^{-1}, respectively, giving a leaf-to-air vapour pressure difference of approximately 1 kPa at 25 °C. A was calculated using Eqn 7.

Time courses of photosynthetic induction were simulated using one set of steady-state photosynthetic parameters. Initial and final steady-state values for V_{cmax} used were V_{cmaxi} = 10 µmol m^{-2} s^{-1} and V_{cmaxf} = 80 µmol m^{-2} s^{-1}, respectively, whereas g_{sci} and g_{scf} were scaled to maintain the same g_{sc}/V_{cmax} ratio at low and high irradiance, akin to maintaining constant C_i at the two steady states (Wong, Cowan, & Farquhar, 1979). The g_{sc}/V_{cmax} ratio used was 2.8 × 10^3 and was the mean ratio of g_{scf} and V_{cmaxf} observed across the data from Deans et al. (2019). R_d was set at zero for simplicity. τ_V was set at 5 min, whereas simulations encompassed values of $\log_{10}(\tau_g/\tau_V)$ between -0.75 and 1.45. Simulated time courses were run for 600 min. $dA(t)$ and $dA_{diff}(t)$ were calculated for each simulation, whereas the relative range for the elimination method (rel. range(ΔC)$_{elim}$; Eqn 18) and the relative error for the differential method (rel.error(ΔC)$_{diff}$; Eqn 35) were also calculated for each simulation for both the one-step and stepwise methods.

3.3 | The effect of boundary layer conductance, ternary correction and consistency in gas exchange equations on limitation estimates

The equations used in most gas exchange systems include both boundary layer conductance and ternary corrections (von Caemmerer & Farquhar, 1981), whereas the gas exchange equations employed in limitation analyses typically ignore their effects (Grassi & Magnani, 2005; Wilson et al., 2000). We wanted to test (1) whether boundary layer conductance and ternary correction have a large impact on the estimation of limitations when the equations used in calculating gas exchange data and limitation analyses are consistent?; and (2) what effect does using gas exchange data and limitation analyses with different assumptions have on the estimation of limitations? To test both questions, simpler forms of the limitation analyses were performed, ignoring either the ternary correction ($E = 0$ in analysis equations) or

both the ternary correction and boundary layer conductance ($E = 0$, g_{tc} = g_{sc} and $g_{tw} = g_{sw}$ in analysis equations). These were tested on gas exchange data that were recalculated to match the assumptions used in the analysis (consistent) or on the full ternary and boundary layer gas exchange data as are usually obtained from gas exchange systems. For the case of ignoring the ternary correction but including boundary layer conductance, total conductance to water vapour was calculated at each time point as

$$g_{tw} = \frac{E}{(VPDL/P_{atm})}, \tag{40}$$

where $VPDL$ is the leaf-to-air vapour pressure difference and P_{atm} is atmospheric pressure, assumed to be 100 kPa.

Stomatal conductance to CO_2 (g_{sc}) was then recalculated as

$$g_{sc} = \frac{g_{bw}g_{tw}}{1.6(g_{bw} - g_{tw})}, \tag{41}$$

and total conductance to CO_2 (g_{tc}) was calculated using Eqn 5. C_i was then recalculated at each time point as

$$C_i = C_a - \frac{A}{g_{tc}}. \tag{42}$$

For the case of ignoring both the ternary correction and boundary layer conductance, total conductance to water vapour was calculated at each time point as

$$g_{sc} = \frac{E}{1.6(VPDL/P_{atm})}. \tag{43}$$

C_i was then recalculated as

$$C_i = C_a - \frac{A}{g_{sc}}. \tag{44}$$

Tests of the effect of gas exchange consistency were performed on the one-step method only.

4 | RESULTS

4.1 | Temporal estimates of absolute limitations

Stomatal and biochemical components of dA were calculated at each time point using the two elimination methods differing by the order in which limitations were removed and the differential method. These were done for both the one-step and stepwise calculations of limitations.

For the one-step calculation of limitations, the removal of stomatal limitation first led to estimates of predominantly biochemical limitation during the early stages of photosynthetic induction, with only a minimal stomatal limitation (Figure 2a,b). In comparison, removal of the biochemical limitation first gave colimitation between stomata and biochemistry of roughly the same magnitude in the early stages of photosynthetic induction (Figure 2a,b). In both elimination methods, the biochemical limitation rapidly decreased beyond the initial period

of photosynthetic induction. However, the two elimination methods differed in the behaviour of stomatal limitation during photosynthetic induction: eliminating the biochemical limitation first produced a monotonically decreasing stomatal component of dA, whereas removing the stomatal limitation first gave a transiently rising stomatal component of dA, followed by a gradual decay in the stomatal component (Figure 2a,b). The differential method produced stomatal and biochemical components of dA with a similar temporal behaviour to the elimination method when the stomatal limitation was removed first, but this example predicted a transiently higher stomatal limitation (Figure 2c,d). The differential method also overestimated dA in the middle section of time courses when the stomatal opening time was slow and was caused by an overestimation of dA_{stom} (Figure 2d). The mean of the two elimination methods on average followed the differential method better than the individual elimination methods when dA_{diff} predicted dA closely, except during the earliest stages of photosynthetic induction, when the mean predicted a higher stomatal limitation than the differential method (Figure 2).

Using the stepwise calculation of limitations led to similar estimates of limitations for the differential method for fast stomatal opening and for the elimination method for slow stomatal opening (Figure 3 c,b). However, there was less consistency in the estimate of limitations when using the elimination methods for fast stomatal opening, with an overestimation of the biochemical limitation when the stomatal limitation was removed first (Figure 3a). The mean of the two elimination methods still produced limitations estimates similar to the differential method. The stepwise calculation of limitations using the differential method also led to near perfect calculation of dA for the case of slow stomatal opening (Figure 3d).

4.2 | Time-integrated relative limitations during photosynthetic induction – comparison of elimination methods with the differential method

The time-integrated relative limitation predicted by elimination and differential methods provided a useful way to compare limitations among time courses of photosynthetic induction. Stomatal limitations estimated from the elimination methods were higher when the biochemical limitation was removed first and vice versa (Figure 4). This was also apparent from inspection of the temporal dynamics of limitations, in particular during the early stages of photosynthetic induction (Figures 2 & 3).

Time-integrated relative limitations from the two elimination methods and their mean were compared with that from the differential method during photosynthetic induction. Using the one-step approach, removal of the biochemical limitation first tended to overpredict the total stomatal limitation compared with the differential method, whereas eliminating the stomatal limitation first led to the opposite occurrence, over the usual range of limitations between 0 and 1 (Figure 4a,b). The mean of the two elimination methods, however, corresponded well with the differential method (Figure 4b). A similar pattern was also observed using the stepwise calculation of limitations, except the overprediction and underprediction of stomatal
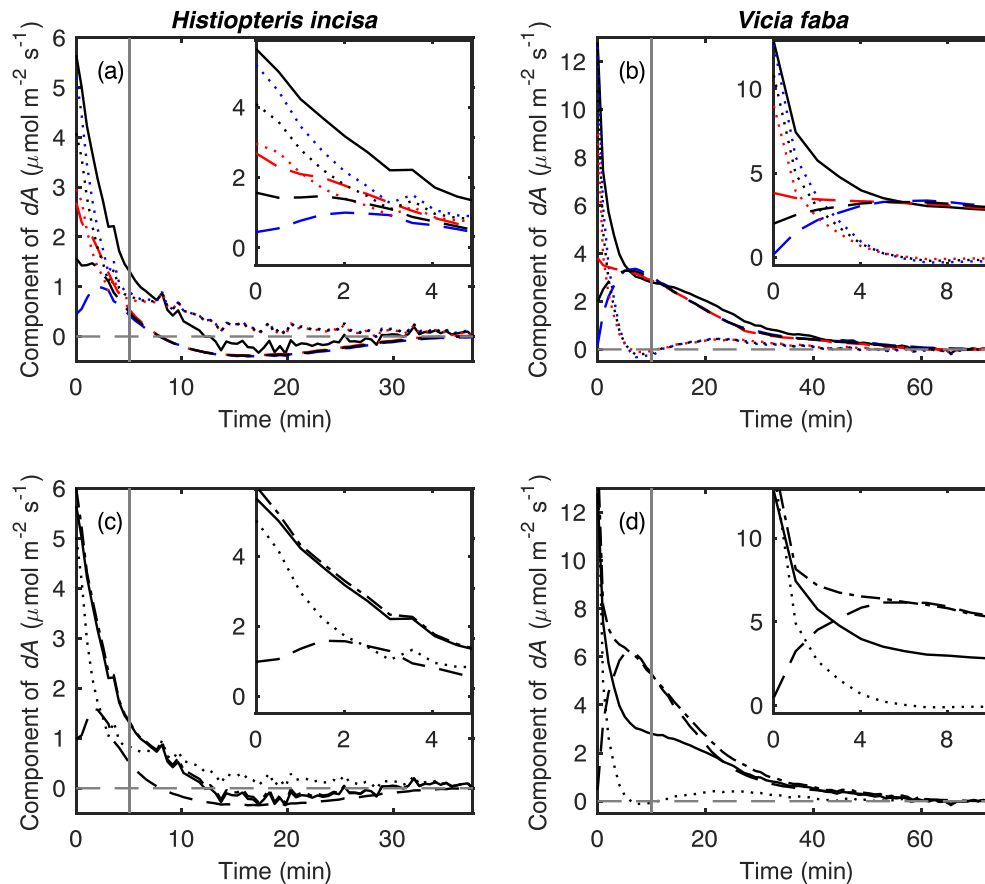
FIGURE 2 Two examples of the one-step calculation of components of dA in *Histiopteris incisa* (a and c; fast stomatal opening) and *Vicia faba* (b and d; slow stomatal opening) using elimination (a and b) and differential (c and d) methods. In all figures, the solid black line is the instantaneous difference in photosynthetic rate (dA). In elimination methods (a and b), Stomatal limitations are shown as dashed lines and biochemical limitations as dotted lines. Red lines represent limitations calculated by removing the biochemical limitation first; blue lines represent removing the stomatal limitation first, and black lines represent the mean of the two. In the differential method (c and d), dashed lines represent stomatal limitations, dotted lines represent biochemical limitations and the dotted-dashed line represents dA estimated from the differential method (dA_{diff}). The initial part of photosynthetic induction is shown in insets. Horizontal grey dashed lines show where dA is zero, and vertical solid grey lines show the maximum time cut-off shown in the insets [Colour figure can be viewed at wileyonlinelibrary.com]

limitations by the elimination method compared with the differential method were greatly exacerbated (Figure 4c). Remarkably, the mean of the two estimates from the elimination method again matched well with that predicted from the stepwise differential method (Figure 4d).

Estimates of limitation estimates between one-step and stepwise differential methods were compared. The two methods compared well, except at stomatal limitations greater than one, where the one-step method under-predicted the limitation compared with the stepwise method (Figure 4e,f).

4.3 | Time-integrated relative limitations during photosynthetic induction - ranges and errors in the estimation of limitations

The reliability of the elimination and differential methods in calculating photosynthetic limitations was assessed by the relative range of the elimination method and the relative error of the differential method, respectively, for both one-step and stepwise calculation of limitations.

Using relative range and error should remove the direct effect of different magnitudes of A, g_{sc} and V_{cmax} on the range and error. In doing so, the key variation should come from differences in the relative rates of biochemical activation (t_{90V}) and stomatal opening (t_{90g}), measured here as durations.

Using the one-step calculation of limitations, relative range in the elimination method was largest when stomatal opening occurred over a timescale similar to that of biochemical activation but reduced as stomatal opening became slower compared with biochemical activation (Figure 5a). In contrast, relative error in the differential method was smallest for small values of t_{90g}/t_{90V}, that is, biochemical activation and stomatal opening occurring at similar rates but rapidly increased as stomatal opening became slower than biochemical activation (Figure 5b).

Using the stepwise calculation of limitations, relative range in the elimination method was very large when stomatal opening and biochemical activation occurred over similar timescales, despite the simulated range being very small (Figure 5c). However, at slow stomatal opening, error was very small. Relative error in the differential
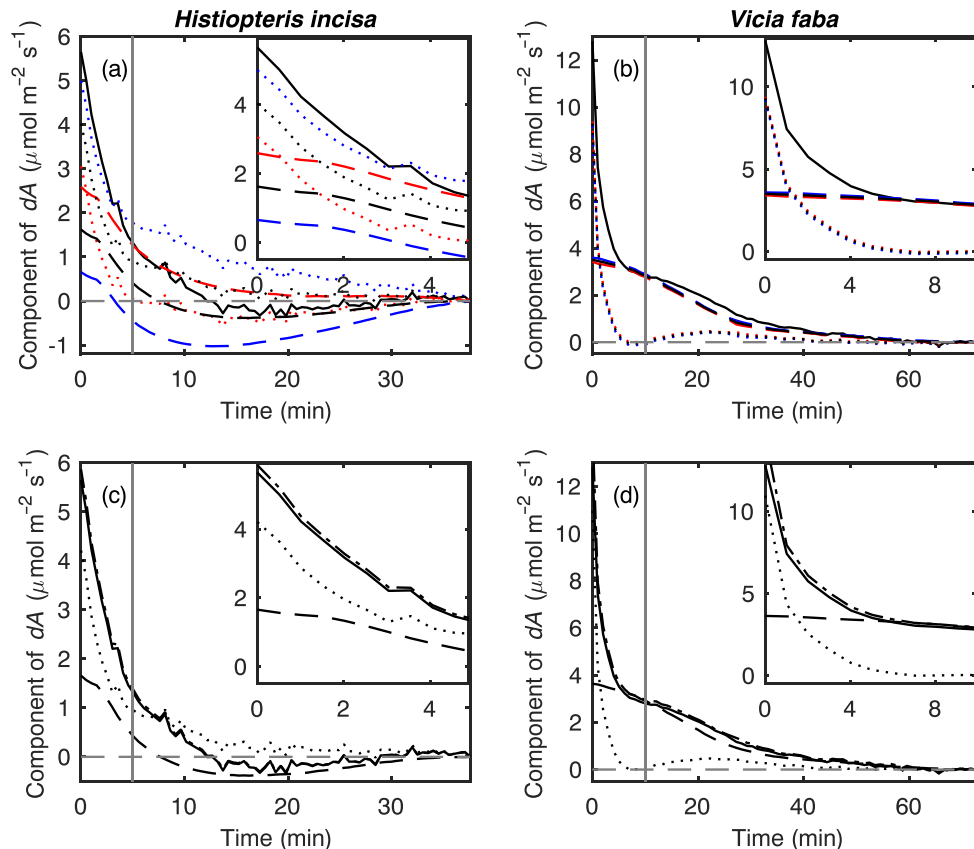
FIGURE 3 Two examples of the stepwise calculation of components of dA in *Histiopteris incisa* (a and c; fast stomatal opening) and *Vicia faba* (b and d; slow stomatal opening) using elimination (a and b) and differential (c and d) methods. In all figures, the solid black line is the instantaneous difference in photosynthetic rate (dA). In elimination methods (a and b), stomatal limitations are shown as dashed lines, biochemical limitations as dotted lines. Red lines represent limitations calculated by removing the biochemical limitation first. Blue lines represent removing the stomatal limitation first, and black lines represent the mean of the two. In the differential method (c and d), dashed lines represent stomatal limitations, dotted lines represent biochemical limitations and the dotted-dashed line represents dA estimated from the differential method (dA_{diff}). The initial part of photosynthetic induction is shown in insets. Horizontal grey dashed lines show where dA is zero, vertical solid grey lines show the maximum time cut-off shown in the insets [Colour figure can be viewed at wileyonlinelibrary.com]

method was predominantly small across the range of t_{90g}/t_{90V} for both observed data and simulations (Figure 5d). However, it is worth noting that because the definition of relative range and error differs between the two methods, a direct, quantitative comparison should be avoided.

4.4 | The effect of boundary layer conductance, ternary correction and consistency in gas exchange equations on limitation estimates

The effect of boundary layer conductance and the ternary correction on estimates of limitations was assessed by comparing the full limitation analyses including ternary and boundary layer conductance limitations against simpler models where both gas exchange data and limitation analyses assumptions were consistent. The comparisons were done for the one-step calculation of limitations only. Provided that the gas exchange data were calculated using similar assumptions to the analyses, predictions using the full and simpler analyses for the elimination method were similar (Figure 6). However, when ternary corrected and boundary layer data were used

in simpler analyses, limitation estimates from the elimination method were inconsistent (Figure 6). In contrast, the differential method appeared immune from these effects and predicted limitations were largely consistent (Figure 6).

5 | DISCUSSION

In response to an increase in irradiance, slow stomatal opening and activation of photosynthetic enzymes leads to plants forgoing photosynthesis compared with instantaneous photosynthetic induction (Deans et al., 2019; Kaiser et al., 2016; Kirschbaum & Pearcy, 1988). Here we estimated the component of forgone photosynthesis corresponding to biochemical or stomatal limitations using two methods: the first sequentially eliminated the effect of each limitation, whereas the second calculated the component of each limitation using a tangent plane approximation. We did this at each time point by a one-step method that did not take into account the path of photosynthetic induction and a stepwise method that used knowledge of future limitations to calculate the current one. We further calculated the contribution each
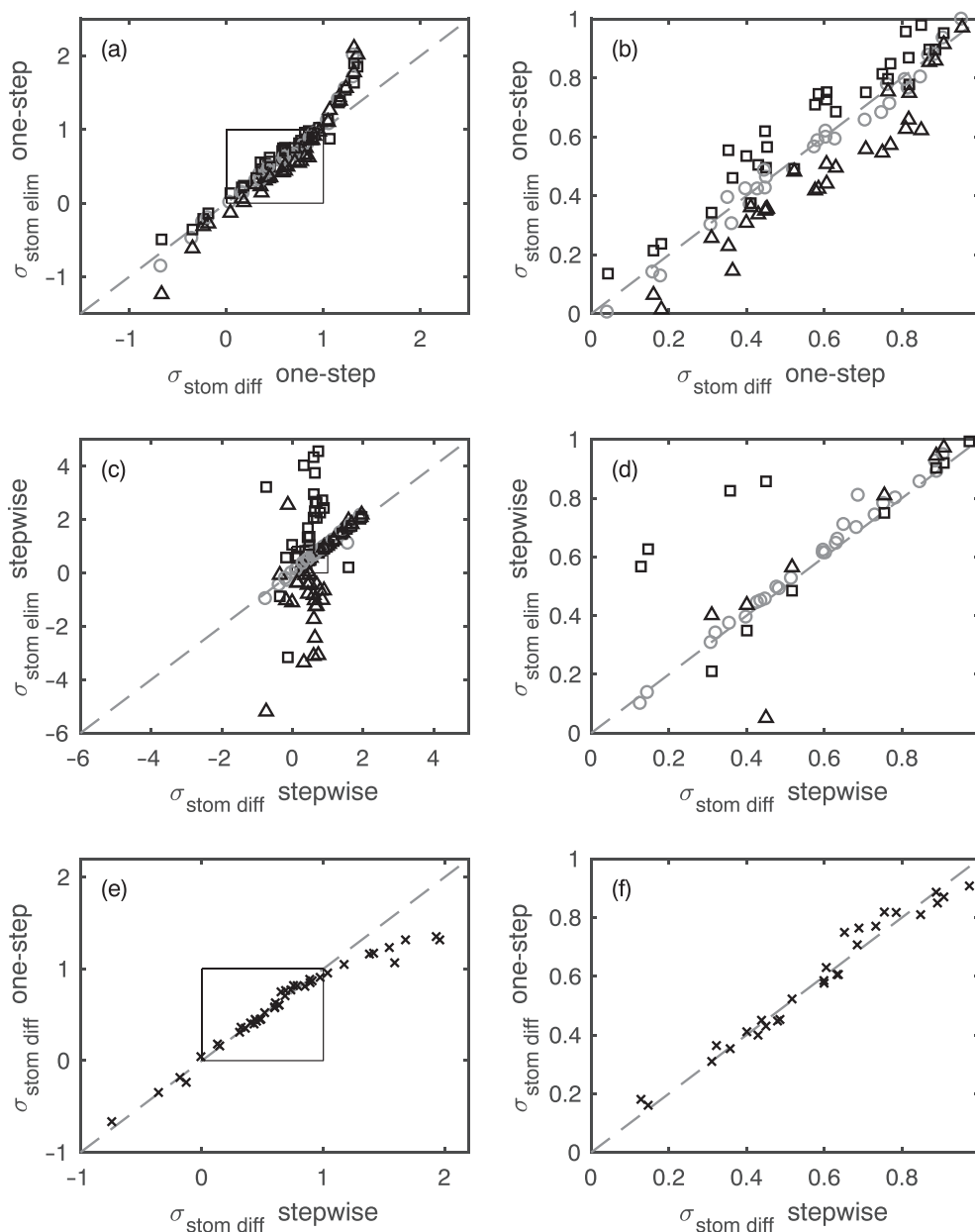
FIGURE 4 Comparison between the time-integrated relative stomatal limitations calculated during photosynthetic induction. (a and b) Comparison of stomatal limitations (σ_{stom}) between the elimination and differential methods using the one-step approach. (c and d) Comparison of stomatal limitations between the elimination and differential methods using the stepwise approach. (e and f) Comparison of stomatal limitations from the differential method, calculated by the one-step and stepwise approaches. Black squares represent limitations calculated by removing the biochemical limitation first, black triangles represent the removal of stomatal limitation first and grey circles represent the mean of the two. (b), (d) and (f) are insets of (a), (c) and (e) around the usual limitation range between 0 and 1. The grey dashed line is 1:1

limitation made to the total potential assimilation forgone and, thus, time-integrated limitations during induction. Each method produces a different estimate for the component of each limitation, raising the question of which method is best to use and when.

We assessed how well each method estimated photosynthetic limitations during photosynthetic induction by considering either the relative range or the relative error of each method. We found that the differential method, when calculated in a stepwise manner, was the best method over a broad range of timescales of biochemical

activation and stomatal opening (Figure 5). This makes intuitive sense, as provided time steps during photosynthetic induction are small enough, then the stepwise differential method is akin to numerically integrating limitations during the induction.

The one-step differential method exhibited a range of relative error from low, when stomatal opening and biochemical activation occurred over similar timescales, to high, when stomatal opening occurred slower than biochemical activation. Given that plants tend to maintain the same C_i across different irradiances at steady state,
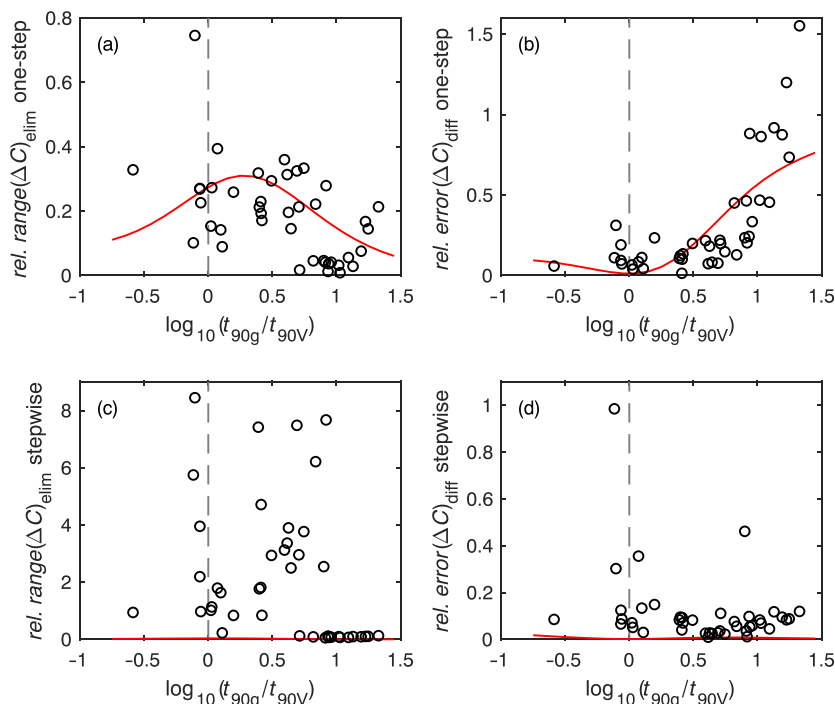
FIGURE 5 Predicted and observed relative range of the elimination methods and relative error of the differential method, for both one-step and stepwise approaches. (a) Relative range in forgone photosynthesis for the elimination method ($rel.range(\Delta C)_{elim}$) using the one-step approach, (b) relative error for the differential method ($rel.error(\Delta C)_{diff}$) using the one-step approach, (c) relative range for the elimination method using the stepwise approach and (d) relative error for the differential method ($rel.error(\Delta C)_{diff}$) using the stepwise approach, all compared with the ratio of stomatal opening to biochemical activation times (t_{90g}/t_{90V}). Open black circles represent actual data, and solid red lines represent modelled relative range or error assuming exponential biochemical and stomatal kinetics and constant internal CO_2 concentration (C_i) at initial and final states. Grey dashed lines show when biochemical activation and stomatal opening occur at the same rate [Colour figure can be viewed at wileyonlinelibrary.com]

stomatal opening and biochemical activation occurring over similar timescales is equivalent to g_{sc} and V_{cmax} changing proportionally such that g_{sc}/V_{cmax} is the same throughout or C_i constant. One can show analytically that the differential method predicts limitations between two states exactly when g_{sc}/V_{cmax} is constant between the two states, or C_i constant, when R_d is ignored or small (for a proof, see Data S1). This is because A is a homogeneous function (of order 1) of both g_{sc} and V_{cmax} (Farquhar, 1989). That is, if both g_{sc} and V_{cmax} are doubled, then A is also doubled (assuming mesophyll conductance is infinite). This leads to A behaving effectively linearly when g_{sc}/V_{cmax} is constant, so that trajectories of constant C_i on the assimilation surface track linear paths across the surface, despite A being a nonlinear function of g_{sc} and V_{cmax} separately (one such path can be visualized in Figure 1d, when the tangent plane is always tangential to the assimilation surface). Thus, if it is known that C_i or g_{sc}/V_{cmax} is constant between two states, then exact stomatal and biochemical limitations can be calculated. The equivalence of limitation sensitivity (l) and relative limitation (σ) when C_i is constant in Wilson et al. (2000) is also because of this homogeneity. Paths that are further away from constant C_i produce more curvature on the assimilation surface so that the one-step method becomes more error prone, but this is reduced in the stepwise method because slopes are recalculated at each new time point.

How well the elimination methods estimated photosynthetic limitations was more difficult to assess. Here we used a metric, the relative range, that estimated how consistent estimates were between removing stomatal or biochemical limitations first. Although we simulated that the elimination method should be more consistent when calculated using the stepwise approach, the stepwise approach used on actual data was much less consistent than the one-step approach, other than when stomata were very slow to open. It appears that

the elimination method when used in a stepwise fashion was too sensitive to small fluctuations in the gas exchange data. This could occur if over some time points, largely different predictions in limitations were predicted for almost no change in assimilation because of noise.

The one-step method was also more consistent in limitation estimates when stomata were slower. This is equivalent to the change in photosynthesis between states being attributable to one limitation over the other and is in direct contrast to the differential method. The dichotomy regarding best method is fortunate for cases where the intermediate time points between states are not known, as it allows us to utilize the differential method when g_{sc}/V_{cmax} or C_i is relatively constant or to use the elimination method when C_i between the two states is different. This has implications for the calculation of limitations in general, beyond the use for photosynthetic induction. It is also interesting to note that the mean of the elimination methods typically produced limitation estimates that were similar to those predicted by the differential method, even when the individual elimination estimates were far from consistent. This is likely a consequence of the mean value theorem in mathematics.

Methods used to estimate biochemical and stomatal limitations to photosynthesis do not consider the effect of boundary layer conductance or the ternary correction, while also employing gas exchange data that do include their effect (Grassi & Magnani, 2005; Wilson et al., 2000). Inconsistencies between gas exchange data that do include the ternary correction and isotope equations that do not has previously been shown to produce errors (Farquhar & Cernusak, 2012). Here we have shown that provided that gas exchange data and limitation analyses are both calculated assuming consistent equations, the effect of boundary conductance and the ternary correction
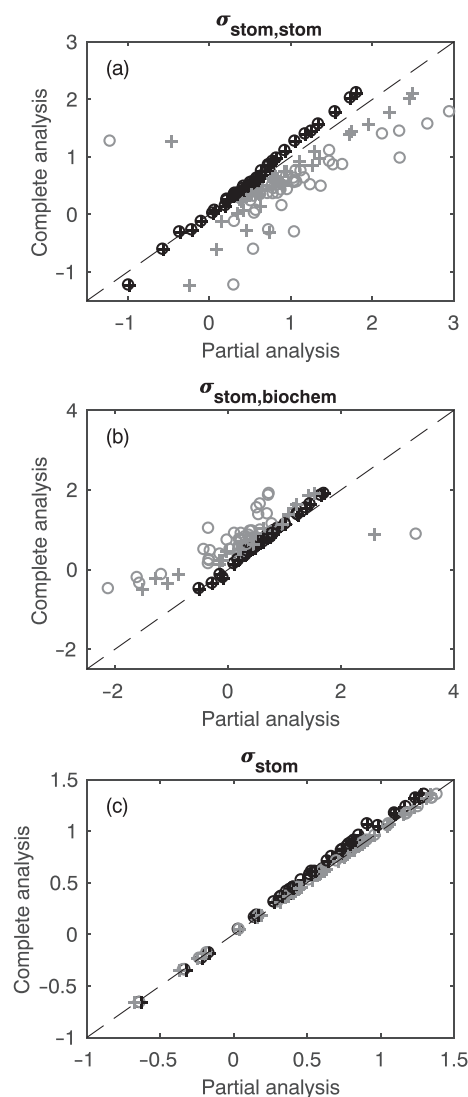
FIGURE 6 Comparisons of stomatal limitation estimates with different gas exchange equations. Complete analysis refers to the relevant limitation analysis with both ternary correction and boundary layer conductance equations, used on data that were calculated also with the ternary correction and boundary layer conductance. Partial analyses are limitation analyses performed using simpler gas exchange equations, on either data that were calculated using the ternary correction and boundary layer conductance (grey) or data that were recalculated to match the gas exchange equations in the analysis (black). Simpler analyses were no ternary correction and no boundary layer conductance (open circle), and no ternary correction but including boundary layer conductance (plus signs). (a) and (b) are elimination methods with (a) stomatal limitation removing stomata first ($\sigma_{stom,stom}$) and (b) stomatal limitation removing biochemistry first ($\sigma_{stom,biochem}$). (d) Stomatal limitations calculated by the differential method (σ_{stom}). Black dashed lines are 1:1 lines

is small for the elimination method. However, if the equations are inconsistent then significant errors in estimates of limitations can occur using the elimination method. In contrast, there was little effect of boundary layer conductance, the ternary correction or consistency of equations on estimates using the differential method. We therefore recommend in particular that if elimination methods are used then the

gas exchange data should be calculated to be consistent with the equations used in the limitations analysis. However, if an adequate number of time points are known then using the differential method is highly encouraged, given the insensitivity of the method to consistency between equations used in the calculation of gas exchange and limitations.

We chose to define a limitation as the difference between two states – the current and the final state. This choice was intuitive for the question that we wanted to ask: of the difference in A from the final A or of total photosynthesis forgone, how much was due to stomatal or biochemical effects? We found that the best representation of temporal limitations during induction was by considering the absolute limitations directly. We also found that defining relative limitations in this way was also the most useful way to describe what proportion of total forgone photosynthesis was due to each limitation. Our definition of σ is similar to that in Wilson et al. (2000). Defining limitations in this way was more intuitive than using a sensitivity limitation, l, (Grassi & Magnani, 2005; Jones, 1985; Wilson et al., 2000). However, relative limitations defined as l may be useful for considering the relative impact on A for relative changes in stomatal or biochemical components. Limitations defined our way are also more realistic than defining limitations relative to completely removing limitations, that is, letting g_{sc} or V_{cmax} be infinite, as described in Farquhar and Sharkey (1982).

CONFLICT OF INTEREST STATEMENT

The authors declare no conflict of interest.

ORCID

Ross M. Deans https://orcid.org/0000-0003-3831-2520
Graham D. Farquhar https://orcid.org/0000-0002-7065-1971
Florian A. Busch https://orcid.org/0000-0001-6912-0156

REFERENCES

Assmann, S. M. (1988). Stomatal and non-stomatal limitations to carbon assimilation: An evaluation of the path-dependent method. *Plant, Cell & Environment, 11*, 577–582. https://doi.org/10.1111/j.1365-3040.1988.tb01799.x

Busch, F. A., & Sage, R. F. (2017). The sensitivity of photosynthesis to O_2 and CO_2 concentration identifies strong Rubisco control above the thermal optimum. *New Phytologist, 213*, 1036–1051. https://doi.org/10.1111/nph.14258

Deans, R. M., Brodribb, T. J., Busch, F. A., & Farquhar, G. D. (2019). Plant water-use strategy mediates stomatal effects on the light induction of photosynthesis. *New Phytologist, 222*, 382–395. https://doi.org/10.1111/nph.15572

Douthe, C., Dreyer, E., Brendel, O., & Warren, C. R. (2012). Is mesophyll conductance to CO_2 in leaves of three *Eucalyptus* species sensitive to short-term changes of irradiance under ambient as well as low O_2? *Functional Plant Biology*, 39, 435–448. https://doi.org/10.1071/FP11190

Douthe, C., Dreyer, E., Epron, D., & Warren, C. R. (2011). Mesophyll conductance to CO_2, assessed from online TDL-AS records of $^{13}CO_2$ discrimination, displays small but significant short-term responses to CO_2 and irradiance in *Eucalyptus* seedlings. *Journal of Experimental Botany*, 62, 5335–5346. https://doi.org/10.1093/jxb/err141

Farquhar, G. D. (1989). Models of integrated photosynthesis of cells and leaves. *Philosophical Transactions of the Royal Society of London. B, Biological Sciences*, 323, 357–367. https://doi.org/10.1098/rstb.1989.0016

Farquhar, G. D., & Cernusak, L. A. (2012). Ternary effects on the gas exchange of isotopologues of carbon dioxide. *Plant, Cell & Environment*, 35, 1221–1231. https://doi.org/10.1111/j.1365-3040.2012.02484.x

Farquhar, G. D., & Sharkey, T. D. (1982). Stomatal conductance and photosynthesis. *Annual Review of Plant Physiology*, 33, 317–345. https://doi.org/10.1146/annurev.pp.33.060182.001533

Farquhar, G. D., von Caemmerer, S., & Berry, J. A. (1980). A biochemical model of photosynthetic CO_2 assimilation in leaves of C_3 species. *Planta*, 149, 78–90. https://doi.org/10.1007/BF00386231

Flexas, J., Ribas-Carbo, M., Diaz-Espejo, A., Galmes, J., & Medrano, H. (2008). Mesophyll conductance to CO_2: Current knowledge and future prospects. *Plant, Cell & Environment*, 31, 602–621. https://doi.org/10.1111/j.1365-3040.2007.01757.x

Grassi, G., & Magnani, F. (2005). Stomatal, mesophyll conductance and biochemical limitations to photosynthesis as affected by drought and leaf ontogeny in ash and oak trees. *Plant, Cell & Environment*, 28, 834–849. https://doi.org/10.1111/j.1365-3040.2005.01333.x

Hermida-Carrera, C., Kapralov, M. V., & Galmés, J. (2016). Rubisco catalytic properties and temperature response in crops. *Plant Physiology*, 171, 2549–2561.

Jarman, P. D. (1974). The diffusion of carbon dioxide and water vapour through stomata. *Journal of Experimental Botany*, 25, 927–936. https://doi.org/10.1093/jxb/25.5.927

Jones, H. G. (1973). Limiting factors in photosynthesis. *New Phytologist*, 72, 1089–1094. https://doi.org/10.1111/j.1469-8137.1973.tb02086.x

Jones, H. G. (1985). Partitioning stomatal and non-stomatal limitations to photosynthesis. *Plant, Cell & Environment*, 8, 95–104. https://doi.org/10.1111/j.1365-3040.1985.tb01227.x

Kaiser, E., Morales, A., & Harbinson, J. (2018). Fluctuating light takes crop photosynthesis on a rollercoaster ride. *Plant Physiology*, 176, 977–989. https://doi.org/10.1104/pp.17.01250

Kaiser, E., Morales, A., Harbinson, J., Heuvelink, E., Prinzenberg, A. E., & Marcelis, L. F. M. (2016). Metabolic and diffusional limitations of photosynthesis in fluctuating irradiance in *Arabidopsis thaliana*. *Scientific Reports*, 6, 31252. https://doi.org/10.1038/srep31252

Kaiser, E., Morales, A., Harbinson, J., Kromdijk, J., Heuvelink, E., & Marcelis, L. F. (2015). Dynamic photosynthesis in different environmental conditions. *Journal of Experimental Botany*, 66, 2415–2426. https://doi.org/10.1093/jxb/eru406

Kirschbaum, M. U. F., & Pearcy, R. W. (1988). Gas exchange analysis of the relative importance of stomatal and biochemical factors in photosynthetic induction in *Alocasia macrorrhiza*. *Plant Physiology*, 86, 782–785. https://doi.org/10.1104/pp.86.3.782

Kromdijk, J., Głowacka, K., Leonelli, L., Gabilly, S. T., Iwai, M., Niyogi, K. K., & Long, S. P. (2016). Improving photosynthesis and crop productivity by accelerating recovery from photoprotection. *Science*, 354, 857–861. https://doi.org/10.1126/science.aai8878

Lawson, T., & Blatt, M. R. (2014). Stomatal size, speed, and responsiveness impact on photosynthesis and water use efficiency. *Plant Physiology*, 164, 1556–1570. https://doi.org/10.1104/pp.114.237107

McAusland, L., Vialet-Chabrand, S., Davey, P., Baker, N. R., Brendel, O., & Lawson, T. (2016). Effects of kinetics of light-induced stomatal responses on photosynthesis and water-use efficiency. *New Phytologist*, 211, 1209–1220. https://doi.org/10.1111/nph.14000

Mott, K. A., & Woodrow, I. E. (2000). Modelling the role of Rubisco activase in limiting non-steady-state photosynthesis. *Journal of Experimental Botany*, 51, 399–406. https://doi.org/10.1093/jexbot/51.suppl_1.399

Slattery, R. A., Walker, B. J., Weber, A. P., & Ort, D. R. (2018). The impacts of fluctuating light on crop performance. *Plant Physiology*, 176, 990–1003. https://doi.org/10.1104/pp.17.01234

Taylor, S. H., & Long, S. P. (2017). Slow induction of photosynthesis on shade to sun transitions in wheat may cost at least 21% of productivity. *Philosophical Transactions of the Royal Society, B: Biological Sciences*, 372(1730), 20160543.

Tazoe, Y., von Caemmerer, S., Badger, M. R., & Evans, J. R. (2009). Light and CO_2 do not affect the mesophyll conductance to CO_2 diffusion in wheat leaves. *Journal of Experimental Botany*, 60, 2291–2301. https://doi.org/10.1093/jxb/erp035

Vico, G., Manzoni, S., Palmroth, S., & Katul, G. (2011). Effects of stomatal delays on the economics of leaf gas exchange under intermittent light regimes. *New Phytologist*, 192, 640–652. https://doi.org/10.1111/j.1469-8137.2011.03847.x

von Caemmerer, S., & Farquhar, G. D. (1981). Some relationships between the biochemistry of photosynthesis and the gas exchange of leaves. *Planta*, 153, 376–387. https://doi.org/10.1007/BF00384257

Wilson, K. B., Baldocchi, D. D., & Hanson, P. J. (2000). Quantifying stomatal and non-stomatal limitations to carbon assimilation resulting from leaf aging and drought in mature deciduous tree species. *Tree Physiology*, 20, 787–797. https://doi.org/10.1093/treephys/20.12.787

Wong, S. C., Cowan, I. R., & Farquhar, G. D. (1979). Stomatal conductance correlates with photosynthetic capacity. *Nature*, 282, 424–426. https://doi.org/10.1038/282424a0

Woodrow, I. E., & Berry, J. (1988). Enzymatic regulation of photosynthetic CO_2, fixation in C_3 plants. *Annual Review of Plant Physiology and Plant Molecular Biology*, 39, 533–594. https://doi.org/10.1146/annurev.pp.39.060188.002533

SUPPORTING INFORMATION

Additional supporting information may be found online in the Supporting Information section at the end of the article.

Data S1: Supporting information